Transactions of the Korean Nuclear Society Spring Meeting
Jeju, Korea, May 7-8, 2015

Visualization Study of Melt Dispersion Behavior for SFR with a Metallic Fuel under Severe Accidents

Hyo Heo [a], Seong Dae Park [a], Dong Wook Jerng [b], In Cheol Bang [a*]
[a]*Ulsan National Institute of Science and Technology (UNIST)*
50 UNIST-gil, Ulju-gun, Ulsan, 689-798, Korea
[b]*Chung-Ang Univ., 84, Heukseok-ro, Dongjak-gu, Seoul 156-756, Korea*
[*]*Corresponding author: icbang@unist.ac.kr*

1. Introduction

In the current Korean sodium-cooled fast reactor (SFR) program, early dispersion of the molten metallic fuel within a subchannel is suggested as one of the inherent safety strategies for the initiating phase of hypothetical core disruptive accident (HCDA). The safety strategy provides negative reactivity driven by the melt dispersal, so it could reduce the possibility of the recriticality event under a severe triple or more fault scenario for SFR [1,2]. Since the behavior of the melt dispersion is unpredictable, it depends on the accident condition, particularly core region. While the voided coolant channel region is usually developed in the inner core, the unvoided coolant channel region is formed in the outer core [3]. It is important to confirm the fuel dispersion with the core region, but there are not sufficient existing studies for them.

From the existing studies [4,5,6], the coolant vapor pressure is considered as one of driving force to move the melt towards outside of the core. There is a complexity of the phenomena during intermixing of the melt with the coolant after the horizontal melt injections. It is too difficult to understand the several combined mechanisms related to the melt dispersion and the fragmentation. Thus, it could be worthwhile to study the horizontal melt injections at lower temperature as a preliminary study in order to identify the melt dispersion phenomena. For this reason, it is required to clarify whether the coolant vapor pressure is the driving force of the melt dispersion with the core region.

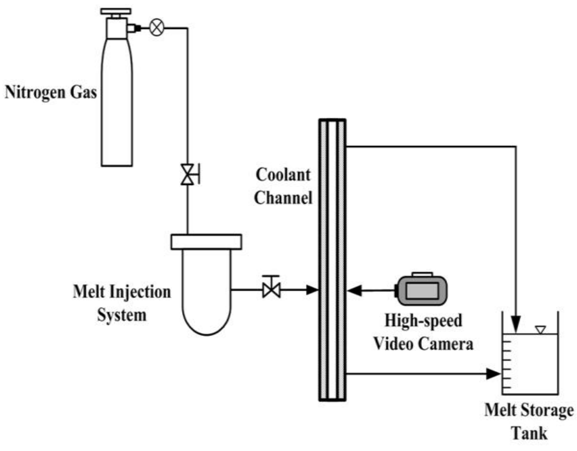

Fig. 1 Scheme of experimental apparatus

In the present study, some experiments were conducted to observe the fundamental dispersion behavior of the melt, which was injected into the coolant channel. For the parametric study, the experiments were performed according to the coolant void condition and the boiling condition. Molten gallium was selected as a simulant material for the metallic fuel (U-20TRU-10Zr) because it is useful to conduct the experiments due to low melting point of the gallium. The molten material was injected into water or R123, which were used as simulants for the coolant. The R123 was used to simulate a coolant boiling condition. The physical properties of molten materials and coolants are listed in Table I, respectively. The materials were selected to reflect a relationship between melting point of melt and boiling point of coolant.

2. Experimental apparatus and experimental conditions

Fig. 1 shows a schematic diagram of the experimental apparatus. The experimental apparatus is composed of a coolant channel to simulate the subchannel structure and a melt injection system. A length between the top end of the coolant channel and the melt injection point is 260 mm. An equivalent inner diameter of the coolant channel is 15 mm, and the inner diameter of the melt injection nozzle is 3.7 mm. One ball valve is installed in the melt injection tube to control the amount of the melt mass. The melt injection into the coolant channel was started by opening the ball valve and terminated by closing the valve. The melt injection mass was measured with a calculation of mass flow rate. Initial temperature and pressure were measured with thermocouples and pressure gauges before the melt injection.

Table I. Physical properties of molten materials and coolants

	Metallic fuel	Gallium	Sodium	Water	R123
Density (kg/m^3)	14100	6095	966	998	1460
Surface tension (N/m)	0.57	0.74	0.20	0.07	0.02
Viscosity (mPa·s)	$5 \cdot 10^{-3}$	$1.89 \cdot 10^{-3}$	1.13	1.00	0.45
Melting / Boiling point (℃)	1077 / -	30 / -	- / 881	- / 100	- / 28

Table II. Experimental conditions

Experimental number	1	2	3	4
Melt temperature (℃)	50	50	50	50
Coolant temperature (℃)	22	22	22	22
Melt injection mass (kg)	1.22	1.61	1.24	1.36
Initial melt injection pressure (MPa)	0.5	0.5	0.5	0.5
Coolant flow velocity (m/s)	0	0	0	0
Coolant saturation (-)	Unvoid	Unvoid	Void	Void
Froude number (-)	1116.1	1230.3	1116.1	1230.3
Weber number (-)	173.1	254.9	173.1	254.9

The melt injection system was pressurized by the nitrogen gas, which determined the initial pressure in the injection system. Visual observation of upward melt dispersion was made through transparent windows of the coolant channel. The dispersion behavior of the molten gallium in the coolant channel was observed, using a high-speed video camera (Phantom, v9.1, 800 frames per second). The time resolution of the images was 0.02 s.

Table II shows experimental conditions. The experimental conditions were set up to get visibility for the melt dispersion behavior. In all cases, the initial melt injection pressure was kept at around 0.5 MPa under zero flow condition. The first case and the second case were intended to confirm the contribution of the build-up vapor pressure in the unvoided coolant channel. The third case was intended to investigate the effect of the coolant void, so the experiment was conducted in the voided coolant channel. The fourth case seemed similar to the third case, but the coolant boiling was considered only in the fourth case.

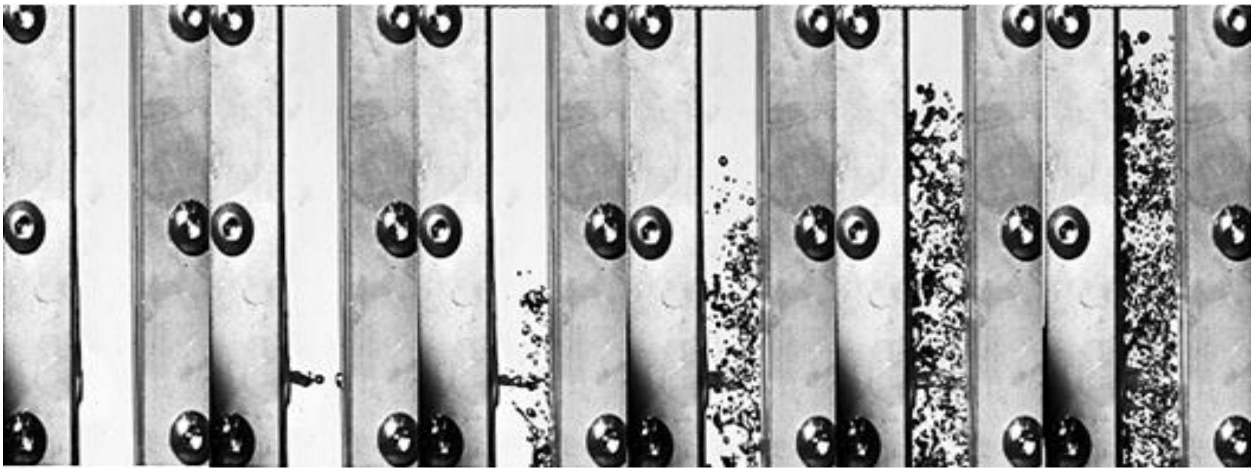

(a)

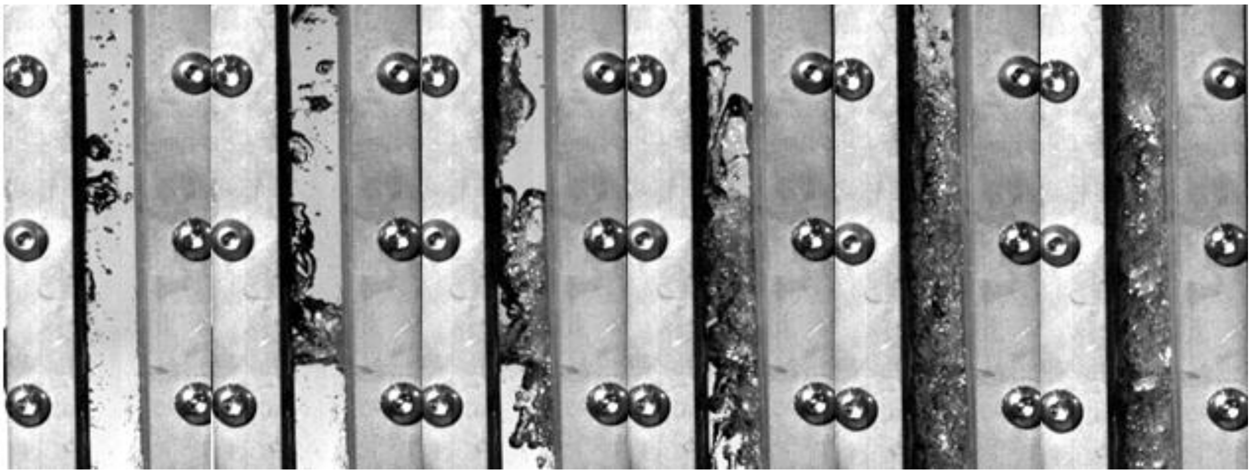

(b)

Fig. 2 Behavior of the melt dispersion in (a) unvoided water channel, and (b) unvoided R123 channel

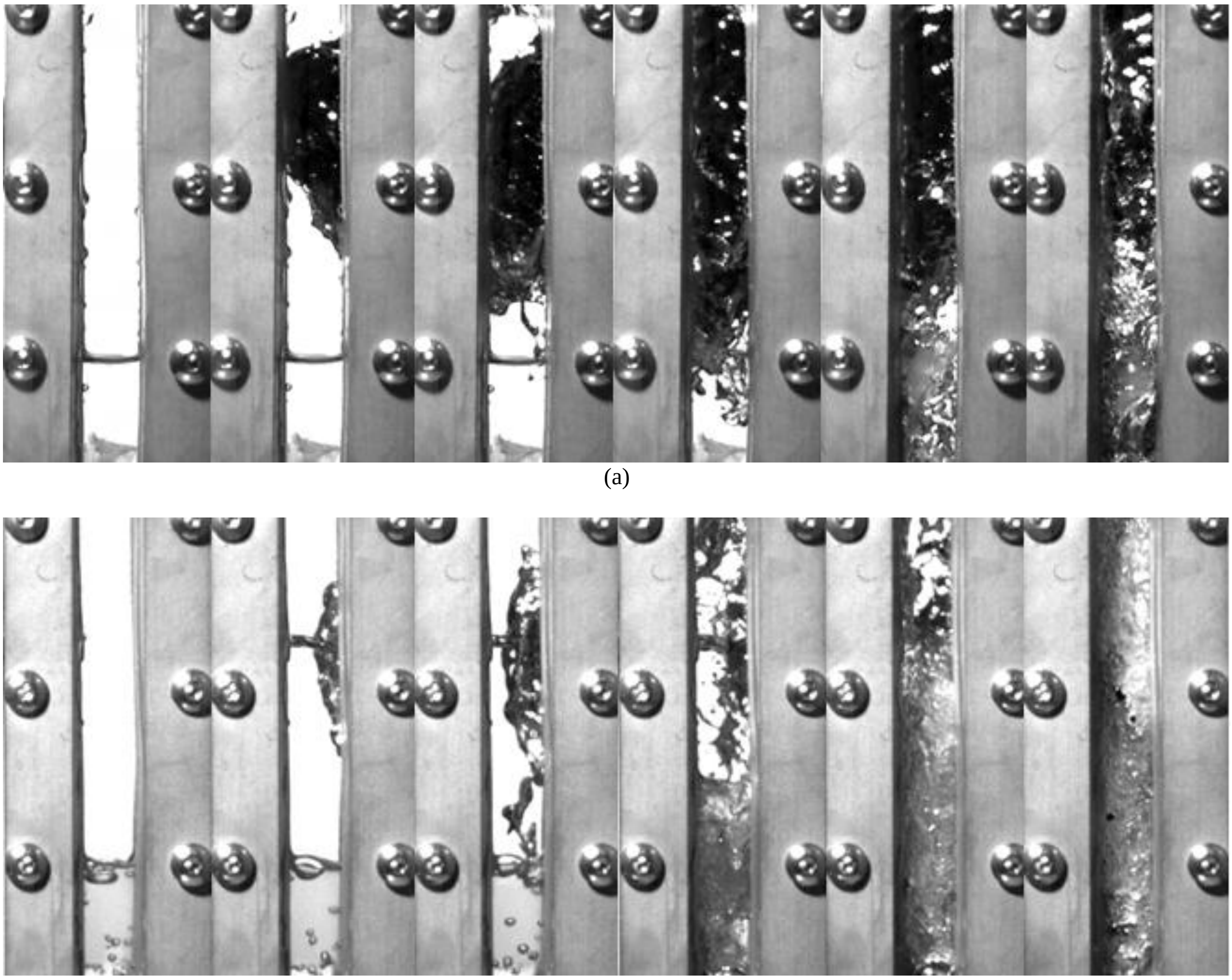

(a)

(b)

Fig. 3 Behavior of the melt dispersion in (a) voided water channel, and (b) voided R123 channel

3. Experimental results

3.1 Unvoided Coolant Channel Region

Fig. 2 shows visual results of the melt injected into the coolant channel under the unvoided coolant condition, which was fully charged coolant into the channel. The beginning behavior of the melt injection of the experiment 1 was identical to that of the experiment 2. The melt was continuously injected by melt injection system. Following the beginning of the melt injection, however, the melt moved upward along with the coolant channel only in Fig. 2 (b). In the experiment 2, coolant boiling started after the beginning of the melt injection. Fig. 2 (b) seemed to show a two phase flow regime where the melt fragments were dispersed upward along with the coolant vapor. The coolant vapor pressure build-up was generated by the contact of the hot melt and the coolant in the voided boundary. The build-up vapor pressure arose in the coolant channel, and then the melt could be discharged upward against gravity. In contrast to the experiment 2, there was not a visible driving force for the upward melt dispersion in the experiment 1. As shown in Fig. 2 (a), the melt was also fragmented into fine particles after the collision with the wall of the coolant channel. The melt was continuously injected into the coolant channel so that a part of the melt seemed to move upward by inertia of the melt. However, the most melt moved downward without refreezing phenomena due to its high-density.

3.2 Voided Coolant Channel Region

Fig. 3 shows visual results of the upward melt dispersion, which was observed under the voided coolant condition. There was the initial injection pressure of 0.5 MPa in these experiments. The melt collided with the wall of the coolant channel and the most broken melt moved downward due to gravity. Although there was no remarkable interaction of the melt in the voided coolant region, the melt behavior in experiment 4 was unique shown in Fig. 3 (b). When the melt fell to the coolant which was submerged in the bottom of the channel, the melt-coolant mixing took place in the boundary surface between the melt and the coolant. It led to the establishment of the coolant void in the vicinity of the melt injection site. The coolant void development can be established only after a stable void formation by a sufficient reduction of coolant subcooling in the coolant channel [7,8]. The void development filled the voided coolant region so that the melt in the voided coolant region moved to upper region of the coolant channel. On the other hand, Fig. 3 (a) shows the experimental results for the melt behavior under the non-boiling condition. The melt was not fragmented, and stacked on the bottom of the coolant channel, which means that the molten metallic fuel may be frozen and plugged forming tight blockages in the subchannel.

4. Conclusions

The specific conditions to be well dispersed for the molten metallic fuel were discussed in the experiments with the simulant materials. The each melt behavior was compared to evaluate the melt dispersion under the coolant void condition and the boiling condition. As the results, the following results are remarked:

1. The upward melt dispersion did not occur for a given melt and coolant temperature in the non-boiling range. Over current range of conditions, the behavior of the melt was so static that the melt was not dispersed in the coolant channel.
2. Under boiling condition, the coolant vapor pressure was built up after the melt injection in both unvoided and voided coolant channel. Following the pressure buildup, the melt was upward dispersed well enough. The build-up vapor pressure was one of driving forces for the upward dispersion of the molten materials.

These experimental results support the possibility of the upward dispersion of the molten metallic fuel by the build-up coolant vapor at the initiating phase of HCDA. More experimental works for the upward melt dispersion are required to clarify the melt behavior within coolant channel, including a structure to simulate fuel rod.

REFERENCES

[1] Y. Abe, T. Kizu, T. Arai, H. Nariai, K. Chitose, and K. Koyama, Study on thermal-hydraulic behavior during molten material and coolant interaction, Nuclear engineering and design, Vol. 230, pp. 277-291, 2004.
[2] T. H. bauer, A. E. Wirght, W. R. Robinson, and A. E. Klickman, Behavior of metallic fuel in TREAT transient overpower tests, Argonne National Laboratory, 1998.
[3] I. Sato, Y. Tobita, K. Konishi, K. Kamiyama, J. Toyooka, R. Nakai, S. Kubo, S. Kotake, K. Koyama, Y. Vassiliev, A. Vurim, V. Zuev, and A. Kolodeshnikov, Safety strategy of JSFR eliminating severe recriticality events and establishing in-vessel retention in the core disruptive accident, Journal of nuclear science and technology, Vol.48, no.4, pp. 556-566, 2010.
[4] E. Matsuo, Y. Abe, K. Chitose, K. Koyama, K. Itoh, Study on jet breakup behavior at core disruptive accident for fast breeder reactor, Nuclear engineering and design, Vol. 238, pp. 1996-2004, 2008.
[5] T. N. Dinh, V. A. Bui, R. R. Nourgaliev, J. A. Green, B. R. Sehgal, Experimental and analytical studies of melt jet-coolant interactions: a synthesis, Nuclear engineering and design Vol. 189.1, pp. 299-327, 1999.
[6] K. Matsuba, M. Isozaki, K. Kamiyama, and Y. Tobita, Experimental study on upward fuel discharge during core disruptive accident in JSFR: Results of and out-of-pile experiment with visual observation, The19th International Conference on Nuclear Engineering (ICONE-19), ICONE19-43993, 2011.
[7] K. Matsuba, M. Isozaki, K. Kamiyama, and Y. Tobita, Mechanism of upward fuel discharge during core disruptive accidents in sodium-cooled fast reactors, Journal of engineering of gas turbines and power, Vol. 135, 032901-1, 2013.
[8] Matsuba, K., Imahori, S., and Isozaki, M, Experimental Study on Void Development Behavior in a Simulated Coolant Channel, Proceedings of the 6th International Topical Meeting on Nuclear Reactor Thermal Hydraulics, Paper No. N6P077, 2004.